Izvestiya, Atmospheric and Oceanic Physics

Vol. 23, No. 7, 1987

UDC 551.466.3

Determination of the Temperature Profile of the Surface Layer of Water from Its Microwave Emissions

K. P. GAYKOVICH, A. N. REZNIK, M. I. SUMIN, AND R. V. TROITSKIY

Research Institute of Radiophysics

The results of theoretical and experimental investigation of the radiometric determination of the temperature stratification of the surface layer of water are presented. Remote measurements at wavelengths of 0.8, 3, 9, and 13 cm are used to reconstruct temperature profiles, which are compared with contact measurements.

We know that a nonuniform temperature distribution (the thermal film) generally develops in the surface layer of water [1-5]. The characteristic thicknesses of thermal films range from 0.1 to 1 cm for temperature differences of up to 1-2 K. The temperature profile of the surface layer plays the key role in heat exchange between the ocean and the atmosphere, and measurements are therefore necessary. Such measurements are also needed when studying hydrophysical processes that cause changes in the temperature of the surface layer. Subjects of study may include internal waves, convection and turbulence.

Temperatures in thermal films are usually measured by contact methods. But these methods do not provide rapid information over large areas, they are difficult to use in the presence of waves, and in addition, contact sensors may change the hydrophysical phenomena being studied.

These circumstances are simulating interest in developing remote methods, especially radiometric methods. The physical basis for developing a sounding method for water is the fact that microwave thermal emissions are produced in the water by a layer whose thickness depends on wavelength. As the wavelength increases, the thickness of the layer in which the thermal radiation is produced changes from tenths of a centimeter to several centimeters (or to 1 cm in saline sea water), so that multifrequency measurements can provide information on the temperature at various depths.

Use of radiothermal sounding for water has made it necessary to investigate various specific problems, and in particular problems involving thermal emissions of a strongly absorbing medium, development of methods for solving the inverse problem of reconstructing the temperature profile, development of procedures, and performance of the measurements.

THERMAL EMISSIONS OF A STRONGLY ABSORBING MEDIUM

Thermal emissions of thermally nonuniform media are generally described by means of a ray intensity transport equation. In strongly absorbing media (in particular, water), when $\varepsilon'' \approx \varepsilon'$ in

the complex dielectric constant $\varepsilon = \varepsilon' - i\varepsilon''$, this approach cannot be used, since the concept of ray intensity loses its meaning in such media [6]. We shall study the radio emissions of the half space $z > 0$ filled with a nonuniformly heated conducting medium. We assume $\varepsilon = 1$ for $z > 0$. The thermal emissions of the half space are generated by a fluctuating current $\mathbf{j}^{st}(\mathbf{r})$, where $\langle \mathbf{j}^{st}(\mathbf{r}) \rangle = 0$, and the correlation function between the k and l components of the current is, according to Levin and Rytov, equal to

$$\langle j_k^{st}(\mathbf{r}) j_l^{st}(\mathbf{r}_1) \rangle|_{\substack{z<0 \\ z_1<0}} = \frac{\omega U[\omega, T(z)]}{4\pi^2} \varepsilon'' \delta(\mathbf{r} - \mathbf{r}_1) \delta_{kl}. \qquad (1)$$

Here, $U[\omega, T(z)] = 1/2\,\hbar\omega \mathrm{cth}[\hbar\omega/2kT(z)]$, where $T(z)$ is the vertical temperature distribution for $z > 0$. The intensity $\boldsymbol{I}(\mathbf{n})$ of the emissions from the absorbing half space into the transparent medium in the direction of unit vector $\mathbf{n}$ are expressed in terms of the electric field coherence function at the interface

$$\Gamma(\mathbf{p}_\perp) = \sum_{i=1}^{3} \langle E_i(\mathbf{r}'_\perp, z) E_i^*(\mathbf{r}''_\perp, z) \rangle|_{z=0}, \quad (\mathbf{p}_\perp = \mathbf{r}'_\perp - \mathbf{r}''_\perp)$$

by the equation [6]

$$I(\mathbf{n}) = \frac{c}{8\pi} \frac{k_0^2}{(2\pi)^2} n_z \int \Gamma(\mathbf{p}_\perp) e^{-ik_0 \mathbf{n}_\perp \mathbf{p}_\perp} d^2 p_\perp, \qquad (2)$$

where $k = \omega/c$. By the reciprocity theorem, the electric field of the fluctuation current is

$$E_i(\mathbf{r}) = \sum_{k=1}^{3} \int_{-\infty}^{\infty} d^2 r'_\perp \int_{-\infty}^{0} dz' E_{ik}^0(\mathbf{r}_\perp - \mathbf{r}'_\perp, z, z') j_k^{ст}(\mathbf{r}'_\perp, z'), \qquad (3)$$

where E°_{ik} is the k component of the field at $\boldsymbol{r}'$, produced by a point dipole located at $\boldsymbol{r}$ and oriented parallel to $\mathbf{i}$. We represent E°_{ik} and j_k^{st} as Fourier intervals in the transverse coordinates, then substitute Eq.(3) into Eq. (2), arriving at an equation for the intensity of thermal emission from the half space

$$I_{E,H}(\theta_0) = (1 - |R_{E,H}(\theta_0)|^2) \gamma(\theta_0) \int_{-\infty}^{0} J(z') e^{\gamma(\theta_0) z'} dz'. \qquad (4)$$

Here $R_{E,H}(\theta_0)$ are the Fresnel reflection coefficients of a plane wave with horizontal (E) and vertical (H) polarizations incident from the transparent medium at an angle θ_0 with the normal to the interface; $\gamma(\theta_0) = 2k_0 \,\mathrm{Im}(\sqrt{\varepsilon - \sin^2\theta_0}$; $J(z) = k_0^2 U(z)/4(2\pi)^3$. Note that if we make a spectral expansion of the fields and sources only in positive frequencies, then $J_+(z) = 4J(z) = k_0^2 U(z)/(2\pi)^3$,

which agrees with the well-known equation for the intensity of equilibrium thermal emissions in a vacuum [7].

The intensity (4) differs from the result obtained by solving the transport equation only in the form of the absorption coefficients $\gamma(\theta_0)$. When $\varepsilon'' << \varepsilon' - \sin^2\theta_0$, we obtain from Snell's law $\sin^2\theta_0 \approx \varepsilon' \sin^2\theta$, where θ is the real refraction angle. In this case $\gamma = k_0\varepsilon''/(\sqrt{\varepsilon'}\cos\theta)$, so that Eq. (4) coincides with the solution of the transport equation.

At radio frequencies we may change over from the intensity of the radiation to the brightness temperature, making the changes in Eq.(4) $I(\theta_0) \to T_я(\theta_0)$, $I(z') \to T(z')$. Then the relationship between the temperature profile and the measured brightness temperatures is given by the equation

$$T_b(\theta_0) = (1 - |R_{E,H}(\theta_0)|^2) \int_{-\infty}^{0} \gamma(\theta_0) T(z) \exp[\gamma(\theta_0) z]\, dz. \qquad (5)$$

Note that radiometric measurements are widely used to determine the surface temperature of of water (see, e.g., Swift [8] and Shutko [9]). It is generally assumed that the temperature distribution is homogeneous and that $T(z) = T(0) = T_{surf}$. The surface temperature is defined as

$$T_{surf} = T_b/(1 - |R|^2). \qquad (6)$$

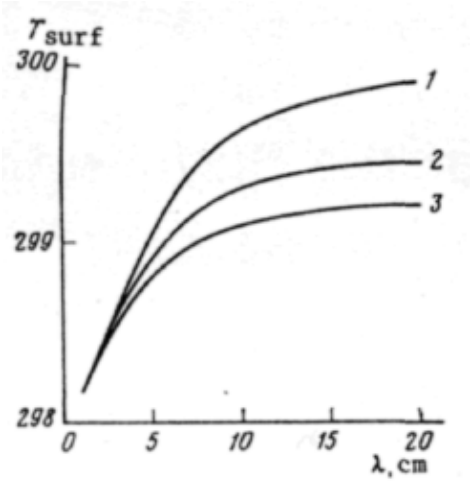

Fig. 1. Plot *of* T_{surf} versus wavelength for profile (7), with T_0 = 300 K, ΔT= -2 K, Δz = 0.3 cm: 1) salinity of water s= 0; 2) s =15‰, 3) s = 30‰.

In the presence of a thermal film, the values of T_{surf} found from Eq.(6) for measurements at various wavelengths will differ from each other and from $T(0)$. Figure 1 shows the plot of T_{surf} versus the wavelength λ for the model temperature profile

$$T(z) = T_0 + \Delta T \exp(-z/\Delta z). \tag{7}$$

In these and subsequent calculations, the dielectric constant ε of water is calculated by the method of Klein and Swift [10]. It is evident from Fig. 1 that the error in determining T in the centimeter region will be comparable to the temperature difference ДГ in the thermal film.

The assumption that the medium is dielectrically uniform, i.e., that $\varepsilon(z) = \text{const}$ ($\gamma(\theta_0)$ in Eq.(5) is independent of ε, is significant in this theory. With a nonuniform temperature profile, this assumption is approximate because there is some dependence on $\varepsilon(T)$, but calculations have shown that the variations are negligible compared with both the direct effect of the temperature profile on the brightness temperature, and with the measurement error.

MEASUREMENT PROCEDURE. FORMULATION AND SOLUTION OF THE INVERSE PROBLEM

Direct use of measured values of T, to solve the inverse problem of reconstructing $T(z)$ is made difficult by the nonlinearity of Eq.(5) with respect to temperature, since the reflection coefficient R has some temperature dependence. The difficulty of solving nonlinear integral equations is well known [11, 12]. In addition, under natural conditions variations in R may result from the presence of waves, foam, pollutant films and the like. Thus, it appears useful to seek for ways of compensating the effect of the reflection coefficient. One method uses compensation with an effective noise signal temperature close to the temperature of the medium under study [13]. We use a different method, based on the fact that the brightness temperature is more sensitive to changes in the water temperature. In this method the effect of R is eliminated by placing the receiving antenna under a metal screen in the nadir direction (see Fig. 2). This approach can be used in laboratory measurements and in field measurements at relatively low altitudes, e.g., from ships or floating platforms. The equation for the brightness temperature at wavelength λ with the effect of R compensated is

$$T_b(\lambda) = \int_{-\infty}^{0} T(z)\,\gamma(\lambda)\exp[\gamma(\lambda)\,z]\,dz, \tag{8}$$

where $\gamma = 2k_0\,\mathrm{Im}(\sqrt{\varepsilon})$ for measurements toward the nadir.

Equation (8) is a Fredholm linear integral equation of the first kind, which is a classic example of an ill-posed problem [11]. Considerable *a priori* information on the exact solution that is sought must be used for numerical solution. This information may vary depending on the specific physical conditions. We solved Eq. (8) by Tikhonov's regularization method [11,12] formulated as a principle of generalized mismatch that incorporates extremely general information on the smoothness of the exact solution. For brevity we rewrite Eq. (8) in the form

(9)

$$AT = T_b^\delta,$$

$$AT \equiv \int_{-a}^{0} T(z)\,\gamma(\lambda)\exp[\gamma(\lambda)\,z]\,dz.$$

$$> c > 0,$$

Here, $a > 0$ is a rather large number, $T_B{}^{\delta}(\lambda)$ is a measured value of the right side, and for a measurement error δ,

where $T_b(\lambda)$ is the right side of Eq. (8) corresponding to the exact solution $T(z)$. According to) of Eq. (8), and thus of Eq. (9), we must minimize on the set of differentiable functions $T(z)$ the functional

$$M^\alpha(T) \equiv \|AT - T_b^\delta\|^2 + \alpha\left(\|T\|^2 + \left\|\frac{dT}{dz}\right\|^2\right), \qquad (10)$$

in which $\|x\|$ designates the norm of the function x as an element of the space of functions that are quadratically summable on the appropriate segment (for a definition of the norm in space L_2 of quadratically summable functions, see, e.g., [11, p. 35]). Here the regularization parameter $\alpha \geq 0$ is the root of a one-dimensional nonlinear equation for the generalized mismatch

$$\rho(\alpha) \equiv \|AT_\alpha - T_b^\delta\|^2 - \delta^2 = 0,$$

(11)

where T_α is a function that minimizes functional (10). Note that in this method of regularizing Eqs. (11) and (10) it is easy to take account of *a priori* information on the nonnegative character

of the exact solution. For this purpose we must minimize functional (10) on the set of non-negative differentiable functions. We note in particular that the case in which we have *a priori* information that the exact solution is greater (or smaller) than all $z \in [-a, 0]$ of some *a priori* function is easily reduced to solution on the class of nonnegative functions. These characteristics of the method enable us to make use of various types of *a priori* information on the exact solution based on the characteristics of the particular physical situation. The problems of minimizing functional (10) reduce, after appropriate discretization, to their finite difference analogs, constituting a problem of quadratic problem, the computations for which have been studied in detail [14].

When we do not know that the exact solution *T(z)* belongs to the compact class of monotonic functions, we can use for solution the appropriate method of Tikhonov et al. [12] which involves minimizing the mismatch

$$\Phi(T) \equiv \| AT - T_b^{\delta} \|^2 \qquad (12)$$

on the set of monotonic functions to a measurement error level of δ^2 (for more detail, see [11, 12]).

We made numerical experiments to establish the most informative spectral region and to formulate requirements regarding the accuracy of measurements and the required number of frequency channels for various distributions *T(z),* varying in their degree of complexity, characteristic thickness, and temperature difference. In addition, from the minimal requirements regarding measurement conditions that were readily implemented, we determined the possible types of profiles *T(z)* that could be reconstructed with sufficient accuracy by the method.

The numerical experiments were made as follows. The values T_b were calculated for various b wavelengths for model profiles *T(z)*. A random number generator was used to discard from the values of T_b the normally distributed error with a zero mean and a variance $(\delta T_b)^2$. The resulting brightness temperature "measurements" were then used to solve the inverse problem. By comparing the reconstructed temperature profile with the initial profile *T(z)*, we can determine the accuracy with which the inverse problem is solved for the specific measurement conditions.

The numerical modeling results indicated that for simple monotonic profiles, good-quality reconstructions were possible with moderate measurement accuracy (0.1 -0.2 K) and with only three wavelengths. With natural films 0.1-1 cm thick, the corresponding optimum wavelengths are 0.3-5 cm for λ_1 , 3-9 cm for λ_2, and 5-15 cm for λ_3. The wavelengths of the measurements increases with the thickness of the film. With a measurement error of 0.1 K, the monotonic pro-

files are reconstructed with an average error of 0.2 K. For salt water, at wavelengths $\lambda > 15$ cm the thickness of the skin layer increases only slightly, limiting the sounding depth for sea water to 1 -2 cm. In fresh water the temperature may be reconstructed in a layer about 10 cm thick. The numerical experiment also showed that high-quality reconstruction of more complex temperature profiles (e.g., with an inversion) measurements must be made with higher accuracy at more frequencies than for monotonic profiles.

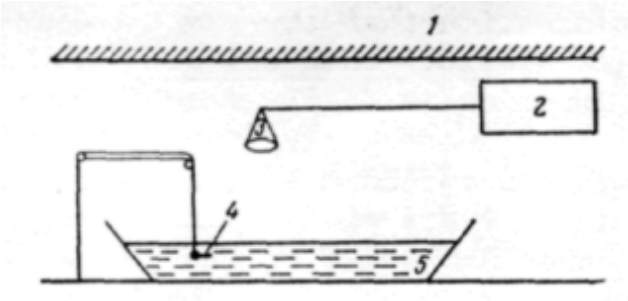

Fig. 2. Layout of laboratory experiment. 1) Metal screen, 2) radiometer, 3) horn antenna, 4) contact temperature sensor, 5) cuvette filled with water.

EXPERIMENTAL STUDY OF TEMPERATURE STRATIFICATION OF THE SURFACE LAYER OF WATER

Our remote method of determining the temperature was realized in a laboratory experiment. The main purpose of the laboratory investigations was to demonstrate the feasibility of the method.

The measurements were made with the radiometer setup diagrammed in Fig. 2. In the first stage, a depth-variable temperature distribution with a characteristic thickness of 1-2 cm and a temperature difference of several degrees was artificially produced in the surface layer of the water. We used a method that enabled us to reproduce this distribution repeatedly. The temperature profile was reconstructed from measurements at wavelengths of $\lambda_1 = 3$ cm, $\lambda_2 = 9$ cm, and $\lambda_3 = 13$ cm. The measurement process included the following:

a) Calibration with uniformly heated water in the cuvette at two temperature values with a temperature difference ΔT approximately equal to the difference between the deep and surface temperatures;

b) Production of a thermal film.

c) Radiometric measurement of the thermal film with integration over periods of 1 to 3 min.

Contact measurements of the temperature profile of the film with a temperature sensor

d) attached to a micrometer screw;

e) Recalibration.

The advantages of this method are that the background radiation is constant during the measurements and calibration and the medium under study is itself used as the calibration standard. This essentially eliminates the main sources of error generally attendant upon absolute radiometric measurements. Under such conditions the measurement error is governed by the fluctuation-al sensitivity threshold of the apparatus for the particular integration time and possible instability of the gain during the measurements. Calibration tests, with allowance for the sensitivity of the radiometers used, indicate that the measurement error δT_b, is a maximum of 0.1 - 0.2 K.

The good agreement between the reconstructed profiles and contact measurements confirmed the description of the development of thermal radio emissions given above, the effectiveness of the algorithms used to solve the inverse problem, and made it possible to estimate the reconstruction error, which was 10 -20% of the temperature difference in the film.

This method can be used to detect changes in the state of the surface thermal film during its alteration over time. Figures 3 and 4 show the results of radiometric measurements and the use of the data to reconstruct the dynamics of the thermal film from its initial state, with a large temperature difference in the thin layer, to the final state with cooling of the film and diffusion into the deeper layers. In this experiment the cooling of the film resulted from contact with air, whose temperature was the same as the temperature in the depths of the water.

Figure 3 shows that at short wavelengths the brightness temperatures are more sensitive to rapid changes in temperature in the thin surface layer, while at long wavelengths the emissions from the deeper, more thermally stable layers are detected. The reconstructions shown in Fig. 4 indicate that the radiometric method allows rather accurate detection of both the decrease in the surface temperature of the film and its diffusion into deeper layers. The algorithms allow the main form characteristics of the temperature profile to be reconstructed with a minimum number of channels.

The results obtained in the first stage of the experimental with artificially produced thermal films make it possible to proceed to the study of natural films arising at the water-air interface as a result of evaporation and heat exchange. The temperature contrast in natural films ranges from fractions of a degree to 1.2 K with a characteristic thickness ranging from tenths of a millimeter to several millimeters. The optimum measurement frequencies for such thin films are in shorter wavelengths, and the required instrument accuracy is increased. We used measurement channels at $\lambda_1 = 0.8$ cm, $\lambda_2 = 3$ cm, and $\lambda_3 = 9$ cm. During calibration, the water in the cuvette was stirred to create a uniformly heated layer. In addition, the cuvette was covered with thin polyethylene film that was transparent to radio emissions. Saturation of the thin layer of air

below the polyethylene film with water vapor prevented evaporation and the formation of a thermal film, which would have been undesirable in the calibration process.

The radiometric measurements were made under various physical conditions that affected the development of the thermal films. The reconstructed temperature profiles and contact measurements are shown in Figs. 5 and 6. It is evident from a comparison of Figs. 5a and 6a that with an increase in the difference between the water and air temperatures, the temperature difference in the thermal film also increases. But evaporation plays a greater role in the development of the cold thermal film. When a fan was used to blow air across the water surface, evaporation increases and the surface cooled rapidly (see Figs. 5b and 6b). This process was directly observable from the radiometric results obtained with the detector. Interestingly, even when hot air was blown across the surface, a cold thermal film occurred: evaporative cooling predominated over heat exchange.

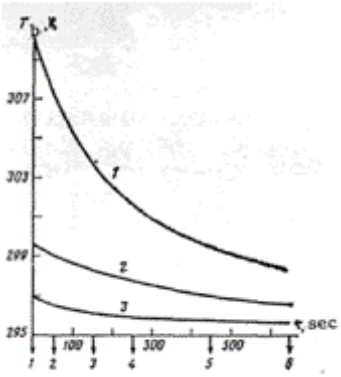

Fig. 3

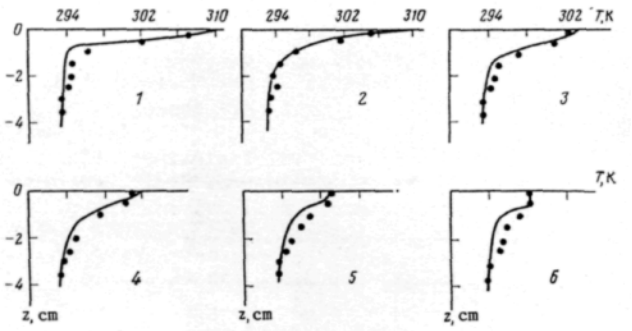

Fig. 4

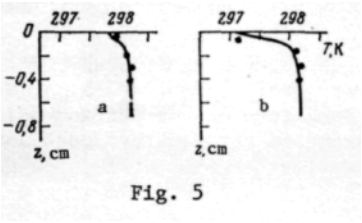

Fig. 5

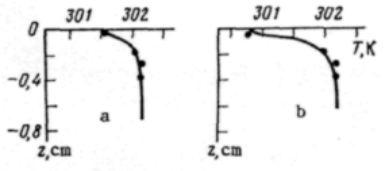

Fig. 6

Fig. 3. Observed time dependence of brightness temperatures of thermal film during cooling and diffusion into depths. Curves 1-3 represent measurements at λ = 3, 9, and 13 cm. Arrows show times at which instantaneous states of thermal film shown in Fig. 4 were reconstructed.

Fig. 4. Reconstruction of thermal film at times shown by arrows in Fig. 3. Circles represent data from contact measurements and solid curves represent reconstructed profiles.

Fig. 5. Reconstruction of natural thermal film from radiometric measurements at 0.8, 3 and 9 cm. Water temperature t_{water} = 25°C, air temperature t_{air} = 22.3°C. Circles represent contact measurements, solid curves represent reconstruction results: a) thermal film without air blown across surface; b) thermal film with air blown across surface with fan.

Fig. 6. Reconstructed curves as in Fig. 5, but for t_{water} = 29°C.

The good agreement between the reconstructed profiles and contact measurements under the different measurement conditions indicated that the radiometric method can be used for remote measurement of the temperature stratification of the surface layer of water under natural conditions.

Received June 23, 1986

REFERENCES

1. Khundzhua, G. G., A. M. Cusev, Ye. G. Andreyev, V. V. Gurov, and N. A. Skorokhvatov. Structure of the Surface Cold Film and Heat Exchange Between the Ocean and the Atmosphere. Izv. AN SSSR. FAO, 13, No. 7, pp. 753-756, 1977.

2. Glnzburg, A. I., A. G. Zatsepin, and K. N. Fedorov. Fine Structure of the Thermal Boundary Layer in Water near the Water-Air Interface. Ibid., 13, No. 12, pp. 1268-1277, 1977.

3. Vershinskiy, N. V., B. N. Nelepo, and A. V. Solov'yev. Mlcrostructure in the Thin Sur face Layer of the Ocean. Dokl. Akad. Nauk SSSR, 247, No. 3, pp. 717-720, 1979.

4. Vershinskiy, N. V., Yu. A. Volkov, and A. V. Solov'yey. Vertical Structure of the Fine Surface Layer of the Ocean. Ibid., 256, No.3, pp. 694-698, 1981.

5. Azizyan, G. V., Yu. A. Volkov, and A. V. So.lov'yev. Experimental Study of the Ther mal Structure of Ocean and Atmosphere Boundary Layers. Izv. AN SSSR. FAO, 20, No.6, pp. 511-519, 1984.

6. Apresynn, L. A. and Yu. A. Kravtsov. Teoriya perenosa izlucheniye (Radiation Transport Theory). Nauka Press, Moscow, 1983, 216 pp.

7. Levin, M. L. and S. M. Rytov. Teoriya ravnovesnykh teplovykh fluktuatsiy v elektrodlnamike (Theory of Equilibrium Thermal Fluctuations In Electrodynamics). Nauka Press, Moscow, 1967, 307 pp.

8. Swift, C. T. Passive microwave remote sensing of the ocean. Boundary-Layer Mete orology, Vol. 18, 1980, pp. 25-54. Shutko, A. M. Investigation of Water Expanses by Microwave Radiometry. Radiotekhnika i elektronika, 23, No. 10, 1978, pp. 2107-2119.

10. Klein, L. A. and C. T. Swift. An improved model for the dielectric constant of sea water at microwave frequencies. IEEE, Vol. AP-25, No. 1, 1977, pp. 104-111.

11. Tikhonov, A. N. and V. Ya. Arsenin. Metody resheniya nekorrektnykh zadach (Methods of Solving Ill-Posed Problems). Nauka Press, Moscow, 1979, 285 pp.

12. Tikhonov, A. N., A. V. Goncharskly, V. V. Stepanov, and A. G. Yagola. Regulyarlziru- yushchiye algoritmy 1 apriomaya Infonnatsiya (Regularization Algorithms and *a Priori* Information). Nauka Press, Moscow, 1983.

13. Troltskiy, V. S., V. A. Aranrhereyev, A. V. Gustov et al. Measurement of the Deep Tem perature Profiles of Biological Entitles from Their Intrinsic Thermal Radio Emissions Izv. vuzov. Radiofizika, 29, No. 1, pp. 62-68, 1986.

14. Pshenichnyy, B. N. and Yu. M. Danilin, Chislennyye metody v ekstremal'nykh zadachakh (Numerical Methods in Extremal Problems). Nauka Press, Moscow, 1975.